ACCURATE ESTIMATION OF INTRACELLULAR DYNAMICS AND UNDERLYING SPATIAL STRUCTURES USING HIERARCHICAL TRAJECTORY SMOOTHING

Ihor Smal[1]*, Niels Galjart*[2]*, Erik Meijering*[1]

Erasmus University Medical Center
[1] Departments of Medical Informatics and Radiology
[2] Department of Cell Biology
P. O. Box 2040, 3000 CA Rotterdam, the Netherlands
Email: i.smal@erasmusmc.nl

ABSTRACT

Biological imaging studies into the molecular mechanisms and underlying structures of intracellular dynamic processes require not only accurate particle tracking but also accurate analysis of the resulting trajectories. Although great efforts have been made to solve the particle tracking problem, there is a lack of methods for robust estimation of dynamic properties from extracted trajectories in the presence of measurement noise, or when particles exhibit jerky motion patterns. Here we propose a hierarchical energy-based trajectory smoothing approach for this purpose. It yields a parametric curve having second-order continuity that allows robust local estimation of dynamic properties requiring up to second-order derivatives at any point along the underlying trajectory. We present preliminary results of experiments on both synthetic and real data of microtubule dynamics demonstrating the advantage of our method over trajectory representations using piecewise-linear connection or Gaussian-process regression.

***Index Terms*—** Trajectory analysis, particle tracking, microtubule dynamics, parameter estimation.

1. INTRODUCTION

Analyzing dynamic properties and underlying spatial structures of moving intracellular objects such as microtubule (MT) tips or vesicles in time-lapse microscopy images is of major interest to many biological studies [1]. An example from our own ongoing research is the study of new chemical compounds for developing novel MT-active drugs that deregulate MT dynamics and prevent mitosis of cancerous cells. This requires robust automated particle tracking and trajectory analysis tools capable of dealing with noisy image data and accurately estimating MT dynamics parameters for assessing drug effectiveness.

Despite great efforts to develop accurate tracking methods [2, 3], particle localization precision is inevitably limited due to imaging noise, confounding the underlying structures along which particles move. Moreover, trajectories are often represented simply by piecewise straight lines between detections, further limiting the accuracy of subsequent analyses [4]. Better results have been obtained recently by using more sophisticated methods such as higher-order B-spline interpolation or Gaussian-process (GP) regression [5]. However, they treat the coordinates independently and rely on the temporal ordering of detections within a trajectory, which in the case of sharp turns may result in overshoots, loops, and unrealistically high curvatures (Fig. 1).

Here we propose a fully adaptive hierarchical energy-based trajectory smoothing method that treats trajectory coordinates jointly as a geometric curve and does not require temporal ordering of detections. The method produces a curve with geometric G^2 and parametric C^2 continuity represented by a set of Hermite polynomials. The strain energy is regularized by penalizing the stretching and bending of the curve, both of which can be related to actual physical properties of the modeled biological structures, and is minimized using quadratic programming. Using the proposed curve representation, properties of interest (curvature, normal and tangent directions, et cetera) can be computed analytically from the resulting curve model, without the need for numerical finite-difference methods.

2. METHOD

2.1. Problem Definition

The proposed method models curves as elastic beams under the application of spring forces. Here, a curve is represented in parametric form using Hermite polynomials, although Bernstein polynomials or B-splines could also serve as a basis. For a trajectory consisting of N_t points $\{(\tilde{x}_t, \tilde{y}_t)\}_{t=1}^{N_t}$, the sought smooth approximating parametric curve $L = L(u)$ is defined by N_e cubic Hermite elements $\{e_k\}_{k=1}^{N_e}$, where

$$e_k = \begin{bmatrix} x_k(u) \\ y_k(u) \end{bmatrix} = \begin{bmatrix} \sum_{i=1}^{4} \phi_i(u) x_i^k \\ \sum_{i=1}^{4} \phi_i(u) y_i^k \end{bmatrix} \qquad (1)$$

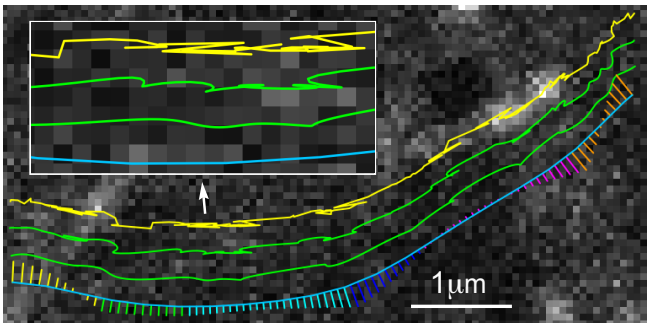

Fig. 1. Single frame from an image sequence depicting jerky motion of fluorescently labeled MT ends at 28°C and one typical (160 frames long) trajectory (yellow overlay). Two estimates of the MT structure obtained with GP regression (using different parameters) exhibit unwanted undulations (green overlays, translated for better visibility). The proposed method estimates the MT as a smooth structure (cyan overlay, where perpendicular lines indicate the amplitude of the curvature along the MT, and different colors represent different elements of the approximating curve).

and $\mathbf{Q} = \{(x_1^k, \ldots, x_4^k, y_1^k, \ldots, y_4^k)\}_{k=1}^{N_e}$ is the set of parameters representing the degrees of freedom of the curve, which defines the coordinates of the beginning and the end of the elements e_k, respectively (x_1^k, y_1^k) and (x_3^k, y_3^k), and the values of the corresponding first derivatives, (x_2^k, y_2^k) and (x_4^k, y_4^k). The Hermite basis functions are defined as

$$\phi_1(u) = 1 - 3(u/h)^2 + 2(u/h)^3 \quad (2)$$

$$\phi_2(u) = h(u/h - 2(u/h)^2 + (u/h)^3) \quad (3)$$

$$\phi_3(u) = 3(u/h)^2 - 2(u/h)^3 \quad (4)$$

$$\phi_4(u) = h(-(u/h)^2 + (u/h)^3) \quad (5)$$

where h is the scale parameter ($0 \leq u \leq h$). Each element e_k has its own scale parameter h_k. Since all N_e elements are sequentially connected, there is a set of $N_e - 1$ linear geometric constraints: $x_3^k = x_1^{k+1}$, $x_4^k = x_2^{k+1}$, $y_3^k = y_1^{k+1}$, $y_4^k = y_2^{k+1}$, $k = 1, \ldots, N_e - 1$, which reduces the number of degrees of freedom to $4(N_e + 1)$.

Reconstructing a smooth curve from a set of trajectory detections is an ill-posed inverse problem, because the uniqueness and stability of the solution are not guaranteed without additional constraints. Therefore, we employ smoothness constraints based on curve derivatives, which turn the curve fitting into a well-posed energy minimization problem:

$$\mathcal{E}(L) = \mathcal{E}_{\text{data}}(L) + \mathcal{E}_{\text{smooth}}(L) = \sum_{t=1}^{N_t} \lambda_t D((\tilde{x}_t, \tilde{y}_t), L)^2 + \sum_{k=1}^{N_e} \left(\int \alpha \left\| e_k' \right\|^2 + \beta \| e_k'' \|^2 + \gamma \| e_k''' \|^2 du \right) \quad (6)$$

where α, β, γ and λ_t are nonnegative weights, and the distance metric D is defined as the shortest Euclidean distance from the object detection to the curve L [6]. The first term controls the fidelity to the data and the second term (potential energy of the curve) controls the smoothness of the solution. The weight λ_t can be used to accommodate the localization accuracy of the object detector and thereby deal with outliers or imprecise detections. The squared first derivative stands for the strain energy due to stretching of the beam, and the squared second derivative stands for the strain energy due to bending. The third derivative does not have a physical analogy but is related to the rate of change of the curvature. Minimizing the integrals in (6) forces the curve to stretch and bend as little as possible. In the case of Hermite polynomials, these integrals can be analytically computed by substituting (1), and rewriting the energy $\mathcal{E}_{\text{smooth}}(L)$ as

$$\mathcal{E}_{\text{smooth}}(L) = \sum_{k=1}^{N_e} \sum_{i=1}^{4} \sum_{j=1}^{4} \kappa_{ij} (x_i^k x_j^k + y_i^k y_j^k) = \mathbf{Q}^T \mathbf{K} \mathbf{Q} \quad (7)$$

where $\kappa_{ij} = \kappa_{ij}^{\alpha} + \kappa_{ij}^{\beta} + \kappa_{ij}^{\gamma}$ are the elements of the stiffness matrix $\mathbf{K} = \mathbf{K}_{\alpha} + \mathbf{K}_{\beta} + \mathbf{K}_{\gamma}$ [6].

2.2. Solving the Nonlinear Optimization Problem

Minimizing the energy in (6) to obtain the smooth curve L is a nonlinear optimization problem that can be solved using successive quadratic programming (SQP) [6]. Here, the quadratic subproblem at each iteration $j = 0, 1, \ldots$ is defined as the minimization (until convergence) of

$$\hat{\mathcal{E}}(\mathbf{d}, \mathbf{Q}^{(j)}) = \mathbf{d}^T \mathbf{K} \mathbf{d} + \nabla \mathcal{E}(\mathbf{Q}^{(j)})^T \mathbf{d} + \tfrac{1}{2} \mathbf{d}^T \nabla^2 \mathcal{E}(\mathbf{Q}^{(j)}) \mathbf{d} \quad (8)$$

using the update vector $\mathbf{d} = \mathbf{Q} - \mathbf{Q}^{(j)}$. This approach results in L having geometric continuity G^1 (the curve elements share the tangent direction at the joints) and parametric continuity C^1 (the first parametric derivatives are continuous). But in order to have a continuous estimate of the curvature, L should be G^2 continuous, and to have a continuous estimate of object acceleration within a trajectory, L should also be C^2 continuous (the one does not necessarily imply the other). To enforce this while at the same time avoiding higher-order polynomials (which are computationally more costly), we constrain the second derivatives:

$$\left. \frac{d^2 e_k}{du^2} \right|_{u=h_k} = \left. \frac{d^2 e_{k+1}}{du^2} \right|_{u=0} \quad (9)$$

for all $k = 1, \ldots, N_e - 1$. This makes the updates $\mathbf{d}$ to be C^2 continuous but not the whole curve described by $\mathbf{Q}$. Thus it is important to use an initialization $\mathbf{Q}^{(0)}$ that is C^2 continuous. In this setup, C^2 implies G^2 continuity.

The scale parameters h_k pertaining to the e_k influence the "flexibility" of L in different parts of the curve. Ideally, to avoid overparametrization of the curve, we would like to have as few elements e_k as possible, with "optimal" h_k. Unfortunately, treating the h_k as extra parameters in the process

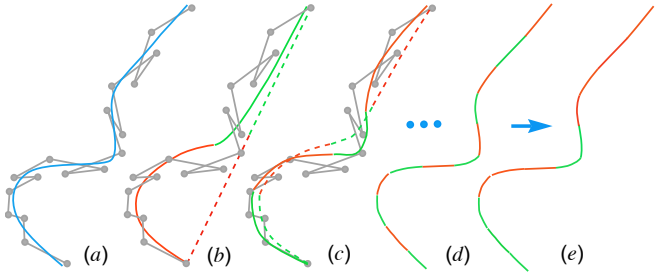

Fig. 2. Illustration of the proposed iterative procedure. (a) The aim is to obtain a smooth parametric curve (blue) from a noisy trajectory (gray). (b-c) For each iteration, the dashed lines represent initializations, and the solid curves represent the improved estimates after the optimization step (here only two colors, green and red, are used to label different elements). After a series of optimization steps (d), partitioning is applied to merge some of the elements and create a curve with an "optimal" number of elements (e).

leads to an intractable optimization problem with no unique solution, unsuitable for SQP. Therefore we propose to use a hierarchical fracturing approach.

2.3. Initialization and Hierarchical Fracturing

The proposed hierarchical approach initializes the curve L using two elements, $L^{(0)} = \{e_1^{(0)}, e_2^{(0)}\}$ with scale parameters $h_1^{(0)} = h_2^{(0)}$, which form a straight line connecting the first and last points of a trajectory (Fig. 2b). For each next iteration $j = 1, \ldots, N_{\text{iter}}$, after running the SQP optimization, each curve element $e_k^{(j-1)}, k = 1, \ldots, N_e^{(j-1)}$, is split into two, if the length of the element $h_k^{(j-1)} \geq 2h_{\min}$ (Fig. 2c). After each iteration, the scales $h_k^{(.)}$ are renormalized to sum up to the curve length. The procedure stops when either a predefined number of iterations, N_{iter}, is reached, or none of the curve elements can be split anymore (Fig. 2d).

In general, splitting an element $e_k^{(j)}$ straightforwardly into two, $e_{k_1}^{(j+1)}$ and $e_{k_2}^{(j+1)}$, with $h_k^{(j)} = h_{k_1}^{(j+1)} + h_{k_2}^{(j+1)}$ and $e_{k_1}^{(j+1)}(h_{k1}^{(j+1)}) = e_{k_2}^{(j+1)}(0)$, may break the C^2 continuity of L at the split point. To alleviate this problem, the parameters $x_3^{k_1}$, $x_4^{k_1}$, $x_1^{k_2}$, $x_2^{k_2}$ and $y_3^{k_1}$, $y_4^{k_1}$, $y_1^{k_2}$, $y_2^{k_2}$ should be recomputed by solving a system of constraining equations:

$$\left.\frac{d^2 e_{k_1}^{(j+1)}}{du^2}\right|_{u=0} = \left.\frac{d^2 e_k^{(j)}}{du^2}\right|_{u=0} \tag{10}$$

$$\left.\frac{d^2 e_{k_2}^{(j+1)}}{du^2}\right|_{u=0.5h_k^{(j)}} = \left.\frac{d^2 e_k^{(j)}}{du^2}\right|_{u=h_k^{(j)}} \tag{11}$$

$$\left.\frac{d^2 e_{k_1}^{(j+1)}}{du^2}\right|_{u=0.5h_k^{(j)}} = \left.\frac{d^2 e_{k_2}^{(j+1)}}{du^2}\right|_{u=0} \tag{12}$$

which leads to a unique solution. Each subsequent splitting provides a more and more accurate initialization for the optimization algorithm in the next iteration, speeding up the overall curve estimation process.

2.4. Optimal Partitioning of Curve Elements

The result of the hierarchical optimization is the curve $L = \{e_1, \ldots, e_{N_e}\}$, $N_e \leq 2^{N_{\text{iter}}+1}$, consisting of multiple small Hermite elements which may heavily overparameterize simple (straight, short, low-curvature) trajectories. In the final step, we seek a more concise representation by combining some of those elements into longer segments (Fig. 2e) while preserving the achieved minimal energy $\mathcal{E}(L)$. To this end we employ a powerful algorithm [7] that searches the exponentially large space of partitions of N data points (curve segments e_k in our case) with complexity $\mathcal{O}(N^2)$. The algorithm is guaranteed to find the global minimum for any energy (fitness) function that is additive in the sense of (6) and automatically determines the number of elements.

The partitioning algorithm replaces blocks of several consecutive elements of L, $e_k, e_{k+1}, \ldots, e_{k+n}$, $k \geq 1, k+n \leq N_e$, with one $\hat{e}_s$, so that $\mathcal{E}(\hat{e}_s) \leq \mathcal{E}(e_k, e_{k+1}, \ldots, e_{k+n})$. In the final partitioning, $\hat{L} = \{\hat{e}_1, \ldots, \hat{e}_{\hat{N}}\}$, the elements $\hat{e}_s$ do not share any of the e_k. By initializing the parameters of $\hat{e}_s$ using the values of $x_1^k, x_2^k, y_1^k, y_2^k$ and $x_3^{k+n}, x_4^{k+n}, y_3^{k+n}, y_4^{k+n}$ we would again break the C^2 continuity of L. To preserve this desired property, we propose to use a higher-order representation, based on quintic Hermite polynomials. Compared to the cubic case this involves two extra basis functions ($\phi_5(u)$, $\phi_6(u)$) and four extra parameters (x_5, y_5, x_6, y_6) that explicitly define the second-order derivatives of a quintic curve element at both ends ($u = 0$ and $u = h$) [6]. Reparameterizaton of L from cubic to quintic Hermite representation is straightforward and preserves the value of $\mathcal{E}(L)$.

To make the final curve representation even more concise, we use an extra energy term in the partitioning process, which corresponds to the Akaike information criterion. It leads to the following fitness constraint during the grouping of the mentioned curve elements into blocks of $\hat{L}$: $\mathcal{E}(\hat{e}_s) \leq \mathcal{E}(e_k, e_{k+1}, \ldots, e_{k+n}) + 2n_{\text{par}}$, where the number of parameters in our case is $n_{\text{par}} = 6(n+1)$. This way, the final partitioning $\hat{L}$ favors a smaller number of elements at the cost of having a slightly higher value of $\mathcal{E}(\hat{L})$.

With the final representation $\hat{L}$, the estimation of all desired parameters such as trajectory length, average speed, tangent and normal components of motion at any point of the trajectory, including curvature and other derived measures, can be easily (and in most cases analytically) computed.

3. RESULTS

3.1. Evaluation on Synthetic Data

The proposed method was first evaluated for speed estimation using the trajectories from the Particle Tracking Chal-

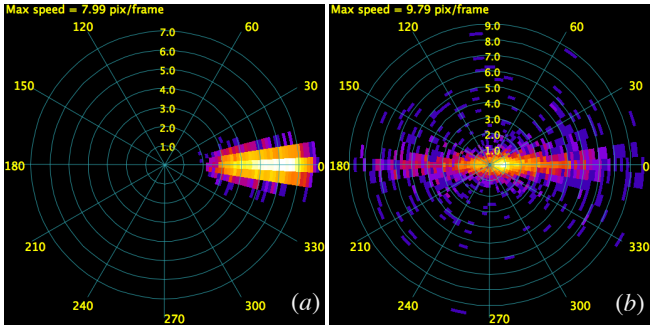

Fig. 3. Polar histogram of the magnitudes and angles (relative to the tangents of L) of the displacement vectors of trajectories. Results are shown for (a) synthetic data (exhibiting processive motion only) and (b) real data from experiments with MTs at 28°C (demonstrating the presence of both processive and retrograde motion).

lenge [2], specifically Scenario 2, which mimics processive motion of MTs. Speed estimates V_{H} were computed for 2,000 trajectories as spatial trajectory length divided by duration, and compared with speed estimates V_{GP} (computed using GP regression), and V_{CUM} (cumulative displacement divided by duration) [5]. The resulting estimates were not very sensitive to the values of the free parameters, which were fixed to $\alpha = 1$, $\beta = 1$, $\gamma = 0.1$, $\lambda_t = 1$, $h_{\min} = 3$ pixels, and $N_{\mathrm{iter}} = 6$. In the case of a perfect object detector, which estimates object locations without errors ($\sigma_d = 0$), the averages were (all in pixels/frame) $\bar{V}_{\mathrm{H}} = 5.25 \pm 0.63$, $\bar{V}_{\mathrm{GP}} = 5.26 \pm 0.68$, $\bar{V}_{\mathrm{CUM}} = 5.29 \pm 0.64$, with the ground truth value $V_{\mathrm{GT}} = 5.22 \pm 0.69$. For a more realistic case ($\sigma_d = 2$ pixels), the averages were $\bar{V}_{\mathrm{H}} = 5.43 \pm 0.68$, $\bar{V}_{\mathrm{GP}} = 5.61 \pm 0.63$, $\bar{V}_{\mathrm{CUM}} = 6.22 \pm 0.61$, with $V_{\mathrm{GT}} = 5.23 \pm 0.68$. This demonstrates that in the case of trajectories without retrograde or jerky motion (Fig. 3a), the proposed method performs as good as or better than the state of the art methods.

3.2. Evaluation on Real Data

To evaluate our method for real applications, we studied the dynamics of wild type MTs, tagged with fluorescent EB3-GFPs at different temperatures (28°C and 40°C, see also Fig. 1), and imaged using a spinning disk confocal microscope. We acquired five image sequences per condition, each sequence containing $\sim$300-700 MTs, whose trajectories were extracted using our MT tracking method [2]. At 40°C, MTs behave as in the case of our synthetic data (Fig. 3a), exhibiting only processive motion with similar distribution of displacements. In this case the speed estimates are in a good agreement with the GP method: $\bar{V}_{\mathrm{GP}} = 2.52 \pm 0.82$ and $\bar{V}_{\mathrm{H}} = 2.45 \pm 0.78$. At the lower temperature, MTs exhibit a lot of retrograde motion (Fig. 3b), resulting in overestimation of speed using GPs: $V_{\mathrm{GP}} = 1.13 \pm 0.57$ versus $\bar{V}_{\mathrm{H}} = 0.56 \pm 0.65$, the latter of which is more accurate according to our experts.

4. DISCUSSION

In this paper we have proposed a fully automated hierarchical curve fitting method for estimating the dynamics of intracellular objects such as MT tips and their underlying MT structure. Contrary to previous trajectory smoothing methods based on cubic B-spline approximation or Gaussian Process regression [5], which require temporally ordered detections, our method is able to better estimate properties of the trajectories of objects showing retrograde or jerky motion. The parametric representation of the obtained curves allows for fast and accurate computation of object speed, trajectory length or curvature, projection of displacements, et cetera. An important advantage of the proposed method is that the estimated parametric curve enables us to characterize object motion along the curve accurately on a very local scale. For example, by extracting the displacement angles and projections onto the tangent directions, we can accurately quantify the proportion of processive and retrograde motion (Fig. 3). The method shows favorable results in our evaluations using synthetically generated trajectories from the Particle Tracking Challenge [2] as well as real data of the behavior of wild-type MTs at different temperatures. Although presented here for 2D+t applications, the proposed approach applies straightforwardly to 3D+t applications. Currently, we are working on an extension of the method using advanced geometric multimodel fitting approaches [8]. This will make it possible to perform simultaneous fitting of multiple curves into single molecule data and reconstructing spatial structures such as actin filaments, microtubules, and neurites.

5. REFERENCES

[1] N. Galjart, "Plus-end-tracking proteins and their interactions at microtubule ends," *Current Biology*, vol. 20, no. 12, pp. R528–R537, 2010.

[2] N. Chenouard et al, "An objective comparison of particle tracking methods," *Nature Methods*, vol. 11, no. 3, pp. 281–289, 2014.

[3] I. Smal and E. Meijering, "Quantitative comparison of multiframe data association techniques for particle tracking in time-lapse fluorescence microscopy," *Medical Image Analysis*, vol. 24, no. 1, pp. 163–189, 2015.

[4] Y. Yao, I. Smal, I. Grigoriev, M. Martin, A. Akhmanova, and E. Meijering, "Automated analysis of intracellular dynamic processes," *Methods in Molecular Biology*, vol. 1563, no. 14, pp. 209–228, 2017.

[5] I. Smal, S. Basu, L. Sayas, N. Galjart, and E. Meijering, "Gaussian processes for trajectory analysis in microtubule tracking applications," in *Proceedings of the IEEE International Symposium on Biomedical Imaging: From Nano to Macro*, 2017, pp. 206–209.

[6] L. Fang and D. Gossard, "Multidimensional curve fitting to unorganized data points by nonlinear minimization," *Computer-Aided Design*, vol. 27, no. 1, pp. 48–58, 1995.

[7] B. Jackson, J. D. Scargle, D. Barnes, S. Arabhi, A. Alt, P. Gioumousis, E. Gwin, P. Sangtrakulcharoen, L. Tan, and T. T. Tsai, "An algorithm for optimal partitioning of data on an interval," *IEEE Signal Processing Letters*, vol. 12, no. 2, pp. 105–108, 2005.

[8] H. Isack and Y. Boykov, "Energy-based geometric multi-model fitting," *International Journal of Computer Vision*, vol. 97, no. 2, pp. 123–147, 2012.